FD 7

Weak Interactions

Elastic Scattering of Neutrinos by Electrons and Protons

David Hedin

State University of New York

Stony Brook, NY, USA

ABSTRACT

Measurements of the cross sections for neutrino and
antineutrino elastic scattering by both electrons and protons are
presented.   These measurements were done at the Brookhaven AGS by
the E734 Collaboration (Brookhaven/Brown/KEK/Osaka/Pennsylvania/
Stony Brook).[1]   These results are then used to determine the weak
mixing angle $\sin^2\theta_w$.

1. Introduction

This paper presents measurements of the cross sections for
neutrino and antineutrino scattering by both electrons and protons.
In the standard electroweak model[2], the ratio of the purely leptonic
weak neutral-current reactions

1

$$\nu_\mu e \rightarrow \nu_\mu e \qquad (1)$$

and

$$\bar{\nu}_\mu e \rightarrow \bar{\nu}_\mu e \qquad (2)$$

is given by

$$R = \frac{\sigma(\nu_\mu e)}{\sigma(\bar{\nu}_\mu e)} = 3 \; \frac{1 - 4\sin^2\theta_W + \frac{16}{3}\sin^4\theta_W}{1 - 4\sin^2\theta_W + 16\sin^4\theta_W} \qquad (3)$$

A measurement of R, which we report in this paper, is used to determine $\sin^2\theta_W$. As many systematic errors in the analysis of the data of reactions (1) and (2) and their normalization cancel in the ratio, the precision of $\sin^2\theta_W$ is primarily determined by the number of events in the two reactions and not by either systematic or theoretical uncertainties.

The nucleon neutral-current reactions

$$\nu_\mu p \rightarrow \nu_\mu p \qquad (4)$$

and

$$\bar{\nu}_\mu p \rightarrow \bar{\nu}_\mu p \qquad (5)$$

depend on the vector and axial vector form factors $F_1(Q^2)$, $F_2(Q^2)$, and $F_A(Q^2)$, and on $\sin^2\theta_W$. The vector form factors are obtained using CVC to express the charged current weak form factors in terms of the proton and neutron electromagnetic form factors measured in electron scattering. If one neglects neutral current contributions from heavy quarks, the axial vector form factor is the same as that determined in quasielastic neutrino scattering ($\nu_\mu n \rightarrow \mu^- p$). Reactions (4) and (5) are correlated with regards to F_A and anticorrelated with regards to $\sin^2\theta_W$. Measuring both reactions

2

anticorrelated with regards to $\sin^2\theta_w$. Measuring both reactions determines both parameters with a limited correlation between $\sin^2\theta_w$ and F_A.

2. Experimental Setup

The neutrino interactions were observed in a massive high resolution target-detector in a broad band neutrino beam of mean energy 1.5 GeV at the Brookhaven Alternating Gradient Synchrotron (AGS). The detector[3] consists of 112 4 m x 4 m modules of liquid scintillator and crossed proportional drift tube (PDT) planes, followed by a shower detector and finally a large aperture muon spectrometer. Each module is about 1/4 radiation lengths long. It possesses energy and angular resolutions for electromagnetic showers of $\Delta E_e/E_e = 0.12/E_e^{1/2}$ and $\Delta\theta = 16$ mrad/$E_e^{1/2}$ with E_e in GeV. For protons, the energy and angular resolutions are 15 MeV and 30 milliradians at a kinetic energy of 250 MeV. Particle separation (electrons from photons and protons from pions) is done using the many dE/dx measurements from the PDT and scintillator cells along the track.

We have collected data from exposures of 2.5×10^{19} and 3.6×10^{19} protons on target for the neutrino and antineutrino phases. This paper will present results from about 40% of the neutrino exposure plus the entire antinuetrino sample for reactions (1) and (2). For the neutrino proton channels ((4) and (5)), we will present results from about 20% and 70% of the neutrino and antineutrino sets respectively.

3. Neutrino - Electron Scattering

Due to the kinematics of the reactions, $E_e \theta_e^2 = 2m_e (1-E_e/E_\nu)$, neutrino electron elastic scattering events are characterized by a single, very forward electron. Backgrounds to the signal consist of (a) photons from π^0 mesons produced in neutral-current reactions, (b) electrons from $\nu_e n \rightarrow e^- p$ or $\bar\nu_e p \rightarrow e^+ n$ induced by the ν_e and $\bar\nu_e$ contaminations in the beam, and (c) a small component of misidentifed low-energy hadrons. The angular distributions of events from these three channels are all approximately flat in θ^2.

Electron were isolated by selecting events with a forward electromagnetic shower with energy between 210 and 2100 MeV. Stringent cuts were then applied to remove showers with extra associated energies. Only showers with less than 30 MeV in the vertex cell were retained. This greatly reduces the ν_e quasielastic background. Furthermore if there was more than 5 MeV in a road upstream of the shower or more than 2 1/2% of the total energy downstream of the vertex and outside a road determined by multiple scattering and the angular resolution the event was rejected. These cuts reduce the π^0 backgrounds significantly with a small (<4%) loss of the signal.

The photon background is further reduced by use of the fact that the energy deposition for electron- and photon-induced showers is markedly different in the first radiation length. Imposing a cut on the ionization loss in the first two proportional drift tube planes and the first calorimeter plane after the vertex yields a sample of primarily singly ionizing events in which approximately

91% of the electrons are retained and only about 35% of the photons
are included. A second sample predominantly containing photons
remains. The distributions in θ_e^2 for these two samples are given
in Fig. 1 for both the ν_μ amd $\bar{\nu}_\mu$-induced data. The electron samples
show a clear peak in the forward direction while the photon
distributions are flat in the forward direction as expected.
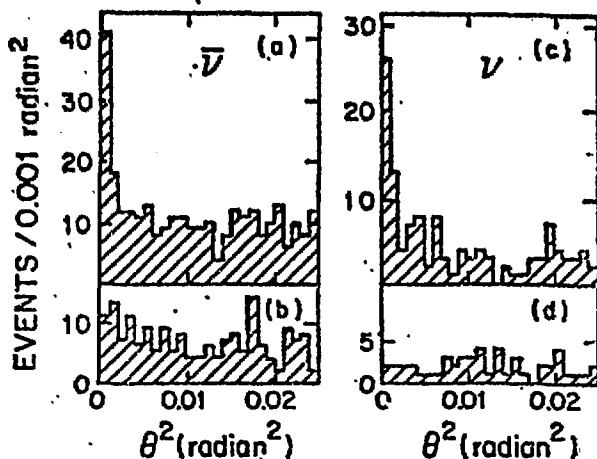Approximately 95% of the signal is expected to lie in the region θ^2
less than 0.01 (radians^2).

FIG. 1. Distributions in θ^2 for (a) the
primarily singly ionizing events from $\bar{\nu}_\mu$
data and (b) the predominantly photon sample
from the $\bar{\nu}_\mu$ data. (c), (d) The corresponding
plots for the ν_μ-induced data.

After background subtraction, which was done fitting the θ^2
distribution to the sum of the background components (taking the

photon and low-energy hadron distributions as flat plus the expected shape of the quasielastic backgrounds (b)), signals of 51 ± 9 and 59 ± 10 remain in the ν_μ and $\bar{\nu}_\mu$ sets respectively. This signal is then corrected for loss of events due to the applied cuts, inefficiencies and due to the fractional ν and $\bar{\nu}$ contaminations in the $\bar{\nu}$ and ν fluxes. To determine the cross sections $\sigma(\bar{\nu}_\mu e)$ and $\sigma(\nu_\mu e)$ and the ratio, we have indirectly measured the integrated incident neutrino fluxes using samples of quasielastic events, $\bar{\nu}_\mu p \rightarrow \mu^+ n$ and $\nu_\mu n \rightarrow \mu^- p$, with small momentum transfer, $0 < Q^2 < 0.4 (GeV/c)^2$. These events were selected by requiring only that the outgoing muon angle with respect to the incident neutrino beam be less than 260 mrad, and that the muon kinetic energy be greater than 0.3 GeV. Events with a visible second track were rejected but no other requirement was placed on the recoiling hadron.

Backgrounds in the normalization samples arise from the presence of charged current single-pion and multipion events. In the $\mu^+ n$ sample single-pion production constitutes 28% of the total sample, while in the $\mu^- p$ sample the corresponding single-pion channels are 31% of the total sample, after detector acceptance is taken into account. Multipion backgrounds are less than 8% of each of the $\mu^+ n$ and $\mu^- p$ total samples, including acceptances factors. This analysis yields the result

$$\sigma(\nu_\mu + e^- \to \nu_\mu + e^-) = [1.60 \pm 0.29 \text{ (stat)} \pm 0.26 \text{ (sys)}] \times$$

$$E_\nu \text{(GeV)} \times 10^{-42} \text{ cm}^2 \qquad (6)$$

and

$$\sigma(\bar\nu_\mu + e^- \to \bar\nu_\mu + e^-) = [1.16 \pm 0.20 \text{ (stat)} \pm 0.14 \text{ (sys)}] \times$$

$$E_\nu \text{(GeV)} \times 10^{-42} \text{ cm}^2. \qquad (7)$$

The ratio of these two values gives

$$R = 1.38 \,^{+0.40}_{-0.31} \text{ (stat)} \pm 0.17 \text{ (sys)}. \qquad (8)$$

The systematic errors were estimated by varying the factors used to determine the corrected electron and normalization samples. Effects studied in the normalization included the Fermi momentum distribution, Pauli exclusion, the value of M_A, the scattering and absorption of pions and nucleons internal and external to the target nucleus, and uncertainties in the cross sections for single-pion and multipion production. Contributions to the systematic error from the electron-photon separation, from electron angular resolution, and from other smaller corrections affecting signal extraction were estimated in the same manner.

This value of R gives

$$\sin^2\theta_w = 0.209 \pm 0.029 \text{ (stat)} \pm 0.013 \text{ (sys)}. \qquad (9)$$

This compares favorably with the only other measurement of the cross section ratio[4] which found $\sin^2\theta_w = 0.215 \pm 0.032 \text{ (stat)} \pm 0.013 \text{ (sys)}$.

Neutrino - Proton Scattering

The signal for $\nu p \rightarrow \nu p$ is a contained track at least three
modules long with ionization consistent with a proton. The vertex
of the event candidates is inside a 2.0 m x 2.0 m x 95 module
fiducial volume. We measure the angle and kinetic energy (by range)
of the track from which one obtains Q^2 and the neutrino energy.

The particle identification technique starts from the end of
the track and compares the actual dE/dx in either scintillator or
PDT to that expected from protons or pions of that residual range
and energy. One then obtains a confidence level for being a proton
or pion idependently in scintillator or PDT. The clear separation
is shown in Figure 2. The efficiency to identify protons has been
measured to be 73% with the losses dominated by nuclear scattering.
The probability of accepting a pion (muon) is less than 2%.
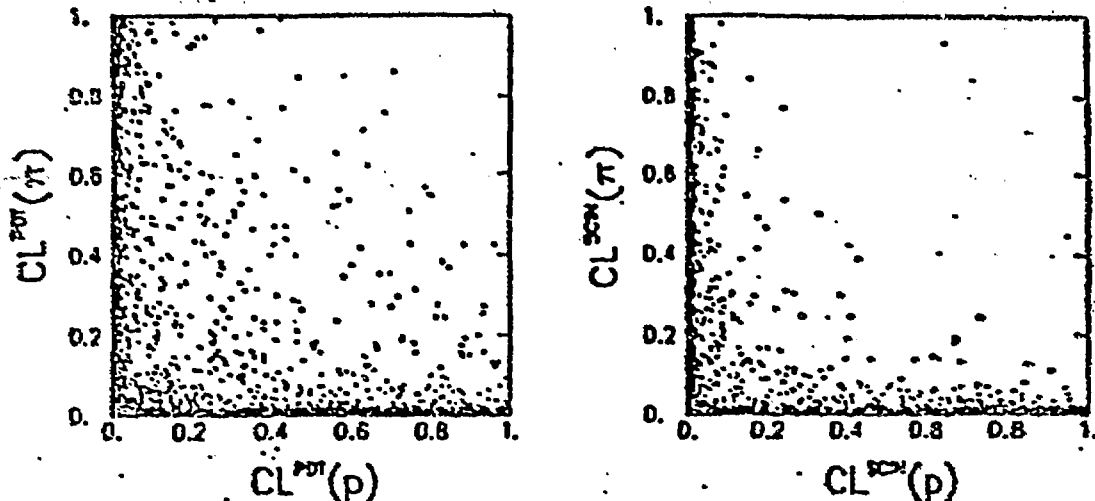
Figure 2. Confidence levels for pion versus proton hypotheseses in
PDT's (left figure) and scintillator (right).

To eliminate events with extra particles (e.g. $\nu n \rightarrow \nu p \pi^-$ or $\nu p \rightarrow \nu p \pi^0$), three cuts are made on the energy depositions in the scintillator: i) the vertex scintillator cell must have less than 50 MeV of visible energy ii) the sum of the energy in a box 3 cells by 3 cells centered on the vertex cell must be less than 110 MeV, and iii) the total energy within five meters of the vertex cell (excluding cells on the tracks) must be less than 20 MeV.

The resulting sample is predominantly $\nu_\mu p \rightarrow \nu_\mu p$ or $\bar{\nu}_\mu p \rightarrow \bar{\nu}_\mu p$. The principal backgrounds are (a) $np \rightarrow np$ events from neutrons which enter the detector, (b) remnant charge current production, (c) neutral current single-pion production, and (d) $\nu_\mu n \rightarrow \nu_\mu n$ where the final state neutron charge exchanges and a proton is detected. The entering neutrons are studied using their event vertex and time distributions. They are found to be about 5% of each sample. Charge current production is only important for the ν sample. It has been determined to be about 5% both by observing the decay of the muon and by Monte Carlo.

The contributions from the other background types are calculated by Monte Carlo. Single-pion events are 9% and 15% of the ν and $\bar{\nu}$ samples. The neutrino neutron elastic scattering (d) is intimately connected to the proton elactic scattering channel and is roughly 17% of the number of elastic proton events. Combining all this, is estimated that about 70% of both the ν and $\bar{\nu}$ sets are due to either $\nu p \rightarrow \nu p$ or $\bar{\nu} p \rightarrow \bar{\nu} p$.

We are currently analyzing data sets in which about 1500 ν and

... ν events satisfy the energy cuts described above. The Q^2 of a
... set of these events is given in Fig. 3. Our acceptance turns on
... about 0.35 $(GeV/c)^2$ due to the minimum length requirement. At
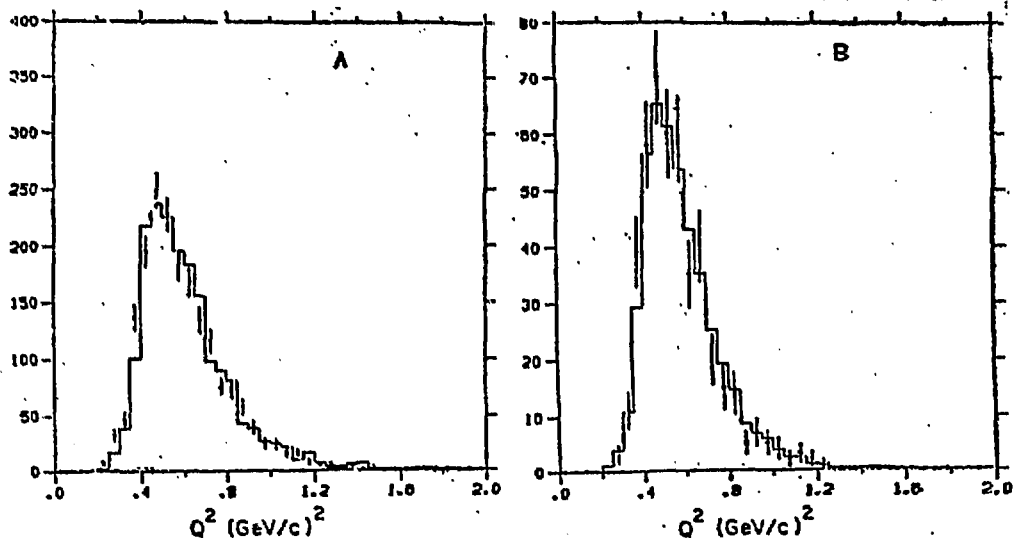... Q^2; the acceptance begins to fall due to both noncontainment
... to interactions.

Figure 3. Distributions in Q^2 for elastic proton candidates for the
ν_μ (A) and $\bar{\nu}_\mu$ (B) date sets. The lines are a Monte Carlo
calculation which combines the signal with the background channels.

The normalization and systematic error procedures used for the
proton signal are similar to that used for the neutrino-electron
sample described in section 3. Preliminary analysis of the ν
sample yield $R_\nu = \sigma(\nu_\mu p \rightarrow \nu_\mu p)/\sigma(\nu_\mu n \rightarrow \mu^- p) = 0.127 \pm 0.006 \pm 0.015$
for $0.4 \leq Q^2 \leq 1.0$ $(GeV/c)^2$. This result represents a statistical

10

$R_\nu = 0.11 \pm 0.015 \pm 0.107$[5] and $R_\nu = 0.11 \pm 0.03$[6].

We are currently completing the analysis on both the ν and $\bar{\nu}$ data sets. This will include studies of the $d\sigma/dQ^2$ of the data and derivations of the weak mixing angle and neutral current form factors.

References

1. K. Abe, L. Ahrens, K. Amako, S. Aronson, E. Beier, J. Callas, P. Connolly, D. Cutts, D. Doughtey, S. Durkin, B. Gibbard, M. Heagy, D. Hedin, J.S. Hoftun, M. Hurley, S. Kabe, R. Lanou, A. Mann, M. Marx, M. Murtagh, S. Murtagh, Y. Nagashima, F.M. Newcomer, T. Shinkawa, E. Stern, Y. Suzuki, S. Tatsumi, S. Terada, D.H. White, H. Williams, T. York.

2. J.E. Kim et al., Rev. Mod. Phys. 53, 211 (1981) and references therein.

3. L.A. Ahrens et al., Phys. Rev. Lett. 51, 1514 (1983),
    L.A. Ahrens et al., Phys. Rev. Lett. 54, 18 (1985).

4.   F. Bergsma et al., Phys. Lett. 147B, 481 (1984).

5.   J. Horstkotte et al., Phys. Rev. D25, 2743 (1982).

6.   P. Coteus et al., Phys. Rev. D24, 1420 (1981).

DISCLAIMER